NASA Technical Memorandum 102010

Second-Order Accurate Nonoscillatory Schemes for Scalar Conservation Laws

Hung T. Huynh
Lewis Research Center
Cleveland, Ohio

Prepared for the
6th International Conference on Numerical Methods in Laminar and Turbulent Flow
cosponsored by the University College of Swansea, UK, Office of Naval Research Branch Office London, International Journal for Numerical Methods in Fluids, International Journal for Engineering Computations, and International Journal for Artificial Intelligence
Swansea, United Kingdom, July 11-15, 1989

NASA

SECOND-ORDER ACCURATE NONOSCILLATORY SCHEMES FOR SCALAR CONSERVATION LAWS

Hung T. Huynh
National Aeronautics and Space Administration
Lewis Research Center
Cleveland, Ohio 44135 U.S.A.

Abstract

A new class of explicit finite-difference schemes for the computation of weak solutions of nonlinear scalar conservation laws is presented and analyzed. These schemes are uniformly second-order accurate and nonoscillatory in the sense that the number of extrema of the discrete solution is not increasing in time.

E-4721

1. Introduction

It is well-known that TVD (total variation diminishing) schemes, see e.g., [4] and the references given there, can give high resolution to discontinuities of the solution. TVD schemes, however, have only first-order accuracy at extrema. Of all second-order accurate TVD schemes, the Minmod scheme is the most diffusive. In [2], Harten and Osher devise the concept of nonoscillatory piecewise-linear reconstruction and modify the Minmod scheme to the UNO2 scheme. Although this latter scheme is uniformly second-order accurate, it retains some of the diffusive character of the former. In this paper, we introduce a new class of schemes, named SONIC, that are uniformly second-order accurate and nonoscillatory.

In section 2, we present TVD and UNO2 schemes from a geometric framework which is rather different from the original presentations. Our description and analysis of these schemes naturally lead to the SONIC schemes later in the section. In section 3, the SONIC schemes are applied to nonlinear scalar conservation laws. It is then shown that the conjecture of Harten and Osher that the midpoint rule is nonoscillatory is indeed correct not only for the UNO2 scheme but also for the SONIC schemes. In section 4, we present some computational results. We note in passing that R. Sanders [3] has recently developed a third-order accurate TVD scheme which degenerates to second-order accuracy near extrema. Our approach, however, is different and appears to be simpler.

2. Advection equation

Consider the initial value problem for the advection equation with constant speed $a > 0$:

$$\frac{\partial u}{\partial t} + a\frac{\partial u}{\partial x} = 0, \tag{2.1}$$
$$u(x,0) = u_0(x).$$

The initial data $u_0(x)$ are assumed to be piecewise smooth functions that are either periodic or of compact support. Let u_j^n be an approximation to the solution u at $x_j = j\Delta x$ and the n-th time level. Equation (2.1) can be discretized in conservation form using the midpoint rule

$$u_j^{n+1} = u_j^n - a\lambda(u_{j+1/2}^{n+1/2} - u_{j-1/2}^{n+1/2}) \tag{2.2}$$

where $\lambda = \Delta t/\Delta x$ and $u_{j+1/2}^{n+1/2}$ is an approximation to u at $x_{j+1/2} = (j+1/2)\Delta x$ and $t^{n+1/2} = t^n + 1/2\Delta t$.

Let $u_{j+1/2}^n$ be an approximation of $u(x_{j+1/2}, t^n)$. The value $u_{j+1/2}^{n+1/2}$ can be approximated by assuming that u^n is linear in $[x_j, x_{j+1/2}]$. (See, e.g., [5].) At time $t^{n+1/2}$, the profile propagates to the right a distance $a\Delta t/2$. The corresponding face value is

$$u_{j+1/2}^{n+1/2} = u_{j+1/2}^n - \tau(u_{j+1/2}^n - u_j^n). \tag{2.3}$$

where $\tau = a(\Delta t/\Delta x)$. Using (2.3), equation (2.2) can be written as

$$u_j^{n+1} = u_j - \tau(u_{j+1/2} - u_{j-1/2}) + \tau^2(u_{j+1/2} - u_j - u_{j-1/2} + u_{j-1}) \tag{2.4}$$

(The superscript n has been omitted here and will be omitted in the remainder of the paper.) Throughout this section, the CFL number is assumed to satisfy $\tau \leq 1$. Our main task is to define the face values $u_{j+1/2}$ from the data u_j. The solution can then be obtained from (2.4).

The following observation is useful for later proofs: let $x(\tau) = x_j - \tau\Delta x$ and $y(\tau)$ =RHS of (2.4). The points $(x = x(\tau), y = y(\tau))$ lie on a parabola P_j as τ varies (Δt varies, a and Δx are fixed). Clearly, the points $U_j = (x_j, u_j) = (x(0), y(0))$ and $U_{j-1} = (x_{j-1}, u_{j-1}) = (x(1), y(1))$ are on this parabola. The tangent T_j to P_j at U_j has slope $(u_{j+1/2} - u_{j-1/2})/\Delta x$, i.e., T_j is parallel to the line $U_{j-1/2}U_{j+1/2}$ where $U_{j-1/2} = (x_{j-1/2}, u_{j-1/2})$. Thus P_j is determined by U_j, U_{j-1}, and T_j. The solution u_j^{n+1} in (2.2) is simply the $y-$component of the point $(x(\tau), y(\tau))$ on the parabola P_j where $0 \leq \tau \leq 1$ as shown in Fig. 1.

2.1 TVD schemes

From a geometric point of view, we describe and prove some important properties of TVD schemes. Let $I(z_1, \ldots, z_k)$ be the smallest closed interval containing $z_1, \ldots, z_k$. Observe that median(x, y, z) lies

in the interval defined by any two of the three arguments. Similarly, median$(z_1, z_2, z_3, z_4, z_5)$ lies in the interval defined by any three of the five arguments, e.g.,

$$\text{median}(x, y, z) \in I(y, z); \quad \text{median}(z_1, \ldots, z_5) \in I(z_1, z_4, z_3) \quad (2.5a, b)$$

To carry out the analysis, it is convenient to define the following central and upwind face values

$$u^c_{j+1/2} = \frac{1}{2}(u_j + u_{j+1}), \tag{2.6}$$

$$u^{up}_{j+1/2} = u_j + (u_j - u^c_{j-1/2}), \tag{2.7}$$

$$u^{up2}_{j+1/2} = u_j + (u_j - u_{j-1}). \tag{2.8}$$

Notice that the Lax-Wendroff scheme corresponds to $u_{j+1/2} = u^c_{j+1/2}$ and the Warming-Beam scheme, to $u_{j+1/2} = u^{up}_{j+1/2}$.

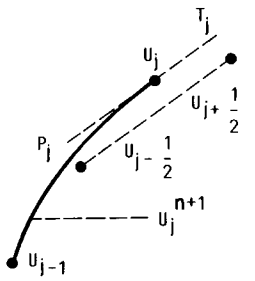

FIGURE 1.

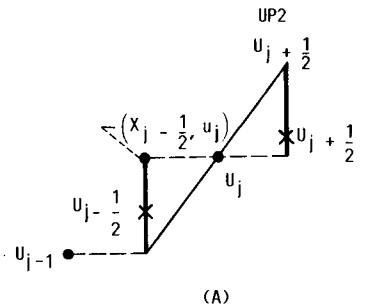

(A)

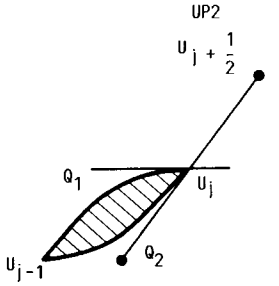

(B)

FIGURE 2.

The Minmod scheme, which is the simplest and the most diffusive of all second-order TVD schemes, can now be described in our framework. The face value for this scheme is

$$u_{j+1/2} = \text{median}(u_j, u^c_{j+1/2}, u^{up}_{j+1/2}). \tag{2.9}$$

For the sake of explaining the terminology, one can observe that

$$\text{minmod}(x, y) = \text{median}(x, y, 0),$$

$$\text{median}(x, y, z) = x + \text{minmod}(y - x, z - x) = y + \text{minmod}(x - y, z - y).$$

The Minmod scheme posesses the following upwind monotonic property

$$u^{n+1}_j \in I(u_j, u_{j-1}). \tag{2.10}$$

To show (2.10), observe that from definition (2.9) and property (2.5a),

$$u_{j-1/2} \in I(u_{j-1}, u^c_{j-1/2}); \quad u_{j+1/2} \in I(u_j, u^{up}_{j+1/2}).$$

Since $u^c_{j-1/2}$ lies between u_{j-1} and u_j, and $u^{up}_{j+1/2}$ lies between u_j and $u^{up2}_{j+1/2}$,

$$u_{j-1/2} \in I(u_{j-1}, u_j); \quad u_{j+1/2} \in I(u_j, u^{up2}_{j+1/2}). \tag{2.11}$$

Properties (2.11) lead to the upwind monotonic property (2.10) by the following reasoning. Another way to state (2.11) is that the point $U_{j-1/2} = (x_{j-1/2}, u_{j-1/2})$ lies on the line segment $(x_{j-1/2}, u_{j-1})(x_{j-1/2}, u_j)$ and $U_{j+1/2}$ lies on $(x_{j+1/2}, u_j)U^{up2}_{j+1/2}$ where $U^{up2}_{j+1/2} = (x_{j+1/2}, u^{up2}_{j+1/2})$. Since the points $(x_{j-1/2}, u_{j-1})$, U_j and $U^{up2}_{j+1/2}$ are on the same line, the slope of $U_{j-1/2}U_{j+1/2}$ lies between 0 and s_2 where $s_2 = \text{slope}(U_j U^{up2}_{j+1/2})$.Because the tangent T_j of the parabola P_j at U_j is parallel to $U_{j-1/2}U_{j+1/2}$ by the observation following (2.4), slope(T_j) also lies between 0 and s_2 (see Fig. 2(A)). Let Q_1, Q_2 be the parabolas though U_j, U_{j-1} such that at U_j, Q_1 has horizontal tangent and Q_2 has tangent of slope s_2. It can be shown that Q_2 has horizontal tangent at U_{j-1} (one can show this by using a linear change of coordinates such that $U_{j-1} = (0,0)$ and $U_j = (1,1)$). Q_1, Q_2 form the boundary of the shaded region in Fig. 2(B). Since P_j also goes through U_{j-1}, U_j and at U_j, its tangent lies between that of Q_1, Q_2, one can derive that the parabola P_j lies in the above shaded region. This completes the proof.

Roe's Superbee scheme can be interpreted in our framework as follows: The face value for this scheme is

$$u_{j+1/2} = \text{median}(u_j, u^c_{j+1/2}, u_{j+1}, u^{up}_{j+1/2}, u^{up2}_{j+1/2}). \tag{2.12}$$

The Superbee scheme is also upwind monotonic, that is, it satisfies property (2.10). To show this, observe that from (2.5b),

$$u_{j-1/2} \in I(u_{j-1}, u^c_{j-1/2}, u_j); \quad u_{j+1/2} \in I(u_j, u^{up}_{j+1/2}, u^{up2}_{j+1/2}). \tag{2.13}$$

As in the Minmod case, $u^c_{j-1/2}$ lies between u_{j-1} and u_j, $u^{up}_{j+1/2}$ lies between u_j and $u^{up2}_{j+1/2}$, thus (2.10) follows.

To describe TVD schemes in general, let

$$r = (u_j - u^c_{j-1/2})/(u^c_{j+1/2} - u_j); \quad R = (u_j - u_{j-1})/(u_{j+1} - u_j), \tag{2.14a,b}$$

(see [4]). From definition (2.6), $r = R$. (However, this will not be the case later when we redefine $u^c_{j+1/2}$.) The face value $u_{j+1/2}$ is obtained by using a limiter function ϕ

$$u_{j+1/2} = u_j + \phi(r)(u^c_{j+1/2} - u_j). \tag{2.15}$$

The first-order upwind scheme corresponds to $\phi = 0$, the Lax-Wendroff scheme to $\phi = 1$, and the Warming-Beam scheme to $\phi = r$.

FIGURE 3.

Next, it is shown that the fact that ϕ satisfies the TVD condition is equivalent to the fact that the face value in eq. (2.15) satisfies properties (2.11). Indeed, the first half of (2.11) with index j replaced by index $j+1$ is $u_{j+1/2} \in I(u_j, u_{j+1})$.This is equivalent to the condition $0 \leq \phi(r) \leq 2$ for all r. The second half of (2.11) is equivalent to $\phi(r) \in I(0, 2r)$. Thus (2.11) is equivalent to the condition that ϕ lies in the intersection of the above two regions, which is the shaded region and the negative r-axis of Fig. 3(A). This is the TVD region as defined by Sweby [4]. Since the Lax-Wendroff and the Warming-Beam schemes are both second-order accurate, to assure second-order accuracy away from extrema, the face value must lie between those of Lax-Wendroff and Warming-Beam,i.e., $\phi(r) \in I(1, r)$. The intersection of this region and the TVD region is named the TVD2 region and is shown in Fig. 3(B). Observe that the upper boundary of the TVD2 region corresponds to the Superbee scheme, and the lower, to the Minmod scheme.

2.2 UNO2 schemes

To resolve the problem of first-order accuracy at extrema of TVD schemes, Harten and Osher developed the UNO2 scheme in [2]. From our point of view, this scheme is the same as the Minmod scheme except that the central face value $u^c_{j+1/2}$ is now obtained by a nonoscillatory quadratic interpolation.

Let Q_j be the parabola through U_{j-1}, U_j, and U_{j+1}. Since Q_j and Q_{j+1} have two points in common, they are either identical or have no other point in common. In the interval $[x_j, x_{j+1}]$, consider the three curves Q_j, Q_{j+1} and the line segment U_jU_{j+1}. Let $Q_{j+1/2}$ be the curve which lies between the other two (Fig. 4). Let $U^c_{j+1/2} = (x_{j+1/2}, u^c_{j+1/2})$ be the intersection of the two tangents to $Q_{j+1/2}$ at U_j and U_{j+1} (notice the x location). An easy calculation yields the central face value

$$u^c_{j+1/2} = \frac{1}{2}(u_j + u_{j+1}) - \frac{1}{4}D_{j+1/2}. \tag{2.16}$$

where

$$D_j = u_{j-1} + u_{j+1} - 2u_j; \quad D_{j+1/2} = \text{minmod}(D_j, D_{j+1}), \quad (2.17a, b)$$

Having defined $u^c_{j+1/2}$, the face value of the UNO2 scheme can readily be obtained from eqs. (2.7) and (2.9).

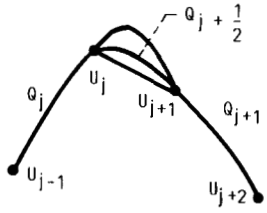

FIGURE 4.

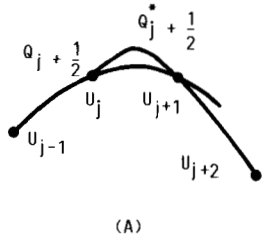

(A)

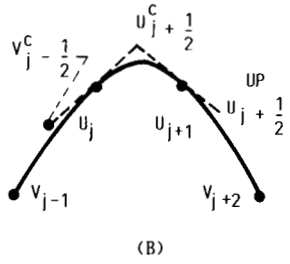

(B)

FIGURE 5.

The first essential property of this scheme is that the interpolation (2.17), (2.16) is nonoscillatory in the following sense: If $u^c_{j+1/2}$ is a strict local maximum (similarly for minimum), i.e., $u_j < u^c_{j+1/2}$ and $u_{j+1} < u^c_{j+1/2}$, then the data (u_k) has a strict local maximum at x_j or x_{j+1}, i.e., $u_{j-1} < u_j$ and $u_{j+2} < u_{j+1}$. To prove this, observe that since $u^c_{j+1/2}$ is a strict local maximum, the parabola $Q_{j+1/2}$ is concave down with the maximum value lying between x_j and x_{j+1}. At least one of the two points U_{j-1}, U_{j+2} lies on this parabola. If both of them belong to $Q_{j+1/2}$, the above claim follows. If only one of them lies on $Q_{j+1/2}$, then the other point belongs to the parabola $Q^*_{j+1/2}$ which lies above $Q_{j+1/2}$ in the interval (x_j, x_{j+1}) by definition. Since two different parabolas can have at most two points in common, $Q^*_{j+1/2}$ lies below $Q_{j+1/2}$ outside of $[x_j, x_{j+1}]$ as shown in Fig. 5(A). This completes the proof. The above property implies that the interpolation procedure does not increase the number of strict local extrema.

The next property of the UNO2 scheme is that if $u^c_{j+1/2}$ is a strict local maximum (similarly for minimum), then

$$u_{j+1/2} = u^c_{j+1/2}; \quad u_{j+3/2} = u^{up}_{j+3/2}. \tag{2.18a,b}$$

Indeed, let $V_{j-1} = (x_{j-1}, v_{j-1})$, $V_{j+2} = (x_{j+2}, v_{j+2})$ be on the parabola $Q_{j+1/2}$ (see Fig. 5(B)). From the above proof, $u_{j-1} \le v_{j-1}$ and $u_{j+2} \le v_{j+2}$. Let $V^c_{j-1/2} = (x^c_{j-1/2}, v^c_{j-1/2})$ be on the line $U_j\ U^c_{j+1/2}$. Then $u^c_{j-1/2} \le v^c_{j-1/2}$. This implies (2.18a). As for (2.18b), it follows from $u^c_{j+1/2} \le u^{up}_{j+1/2}$.

Let $RQ_{j-1/2}$ be the range of the parabola $Q_{j-1/2}$ in $[x_{j-1}, x_j]$, that is, the interval formed by the values $Q_{j-1/2}(x)$ where x varies in $[x_{j-1}, x_j]$. We can now show that the UNO2 scheme posesses the following quadratic upwind monotonic property

$$u^{n+1}_j \in I(u_j, u^c_{j-1/2}, u_{j-1}). \tag{2.19}$$

In fact, we will show $u^{n+1}_j \in RQ_{j-1/2}$ which implies (2.19). Observe first that (2.13) holds. If $u^c_{j-1/2}$ is not a strict local extremum then $RQ_{j-1/2} = I(u_{j-1}, u_j)$ and (2.19) follows exactly as in the Minmod case.

If $u^c_{j-1/2}$ is a strict local extremum, say a maximum, then eqs. (2.18a,b) imply that the parabola P_j is precisely $Q_{j-1/2}$. This completes the proof.

A quadratic upwind monotonic scheme is nonoscillatory in the sense that it can not create new strict local extrema. This follows from the nonoscillatory property of the interpolation (2.16), (2.17).

We next show a simple proof of the second-order accuracy of the UNO2 scheme. Denoting $h = \Delta x$, one obtains by using Taylor series expansions,

$$(u^c_{j+1/2} - u_j)/(h/2) = u'_j + O(h^2), \tag{2.20a}$$

$$(u_j - u^c_{j-1/2})/(h/2) = u'_j + O(h^2), \tag{2.20b}$$

$$(u^{up}_{j+1/2} - u_j)/(h/2) = (u_j - u^c_{j-1/2})/(h/2) = u'_j + O(h^2), \tag{2.20c}$$

$$(u_j - u^{up}_{j-1/2})/(h/2) = u'_j + O(h^2). \tag{2.20d}$$

where u' denotes $\partial u/\partial x$. The last expression follows by writing (2.20c) with index j replaced by $j-1$ and then expanding u'_{j-1} and u_{j-1} around x_j. Since the face value $u_{j+1/2}$ must lie between $u^c_{j+1/2}$ and $u^{up}_{j+1/2}$,

$$(u_{j+1/2} - u_{j-1/2})/h = u'_j + O(h^2). \tag{2.21}$$

Thus the scheme is second-order accurate.

We have presented the UNO2 scheme as a modification of the Minmod scheme by redefining $u^c_{j+1/2}$ using eq. (2.16) above. Will the same procedure yield a modification of the Superbee scheme? The answer is yes as will be shown in the next section.

2.3 SONIC (second-order nonoscillatory interpolating conservative) schemes

We combine the names MUSCLE [6] with UNO2 and come up with SONIC. Of all SONIC schemes, the UNO2 scheme above is the most diffusive and the SONIC-B or Sonicbee scheme below is the most compressive. This scheme can be defined by eqs. (2.17a,b), (2.16), (2.8),(2.12), (2.3) and (2.2). It possesses all the properties of the UNO2 scheme that are mentioned above. To prove the second-order accuracy of the Sonicbee scheme, consider the following cases at face $j + 1/2$:

RX1: $u^c_{j+1/2}$ is a strict local extremum, then $u_{j+1/2} = u^c_{j+1/2}$;

RX2: $u^c_{j-1/2}$ is a strict local extremum, then $u_{j+1/2} = u^{up}_{j+1/2}$;

RX3: if neither of the above cases hold and if u_j is a local extremum, in other words, $(u_j - u_{j-1})(u_j - u_{j+1}) \geq 0$, then $u_{j+1/2} = u_j \in I(u^c_{j+1/2}, u^{up}_{j+1/2})$;

RG: if none of the above cases hold, then we are in the regular case of either ascending order $u_{j-1} \leq u^c_{j-1/2} \leq u_j \leq u^c_{j+1/2} \leq u_{j+1}$ or descending order. The case RG1 corresponds to $r = (u_j - u^c_{j-1/2})/(u^c_{j+1/2} - u_j) \leq 1$;

RG2: this is the regular case where $r > 1$.

In any of the above cases, $u_{j+1/2} \in I(u^c_{j+1/2}, u^{up}_{j+1/2})$ and the above claim follows.

The Sonicbee scheme is also quadratic upwind monotonic and the proof is exactly the same as that of the UNO2 scheme. To describe the class of SONIC schemes, we need some more definitions.

At each face $j+1/2$, let the linear upwind monotonic interval $I^1_{j+1/2}$ be the intersection of $I(u_j, u_{j+1})$ and $I(u_j, u^{up2}_{j+1/2})$. Then condition (2.11) is equivalent to $u_{j+1/2} \in I^1_{j+1/2}$, and, as shown in section 2.1, these are equivalent to the TVD condition in [4]. Similarly, let the quadratic upwind monotonic interval $I^2_{j+1/2}$ be the intersection of $I(u_j, u^c_{j+1/2}, u_{j+1})$ and $I(u_j, u^{up}_{j+1/2}, u^{up2}_{j+1/2})$. Then condition (2.13) is equivalent to

$$u_{j+1/2} \in I^2_{j+1/2}. \tag{2.22}$$

Schemes satisfying (2.22) posess the quadratic monotonic property (2.19). The proof is similar to that of the UNO2 scheme and is omitted. Observe that $I^2_{j+1/2}$ is equal to $I^1_{j+1/2}$ except in the cases EX1 and EX2 above where $I^2_{j+1/2}$ strictly contains $I^1_{j+1/2}$. Enlarging $I^1_{j+1/2}$ to $I^2_{j+1/2}$ in these cases permits second-order accuracy at extrema.

Let $I^2_{j+1/2} = I(c_1, c_2)$. Any high-order accurate scheme can be made nonoscillatory by defining

$$u_{j+1/2} = \text{median}(\bar{u}_{j+1/2}, c_1, c_2) \tag{2.23}$$

where $\bar{u}_{j+1/2}$ is the face value of the scheme.

We can now describe the SONIC schemes. Consider first the EX cases. In each of these cases, both the most diffusive (UNO2) and the most compressive (Sonicbee) members give the same face value. Thus all other SONIC schemes must also have the same face value. One can also come to the above conclusion by observing that the intersection of $I(u^c_{j+1/2}, u^{up}_{j+1/2})$ and $I^2_{j+1/2}$, i.e., the intersection of the second-order accurate interval and the quadratic upwind monotonic interval, contains exactly one point. This point must be the face value of all SONIC schemes.

Next, consider the regular case. In the cases RG1, RG2 above,

$$I^2_{j+1/2} = I(u_j, u^{up2}_{j+1/2}), \quad I^2_{j+1/2} = I(u_j, u_{j+1}) \tag{2.24a,b}$$

respectively. Let $\phi(r)$ be a continuous function for $r > 0$. With $u^{\phi}_{j+1/2}$ defined by eq. (2.15), using (2.23) and (2.24a,b), one obtains

$$u_{j+1/2} = \text{median}(u^{\phi}_{j+1/2}, u_j, u^{up2}_{j+1/2}), \tag{2.25a}$$

$$u_{j+1/2} = \text{median}(u^{\phi}_{j+1/2}, u_j, u_{j+1}) \tag{2.25b}$$

respectively. Schemes defined as above are nonoscillatory. They are second-order accurate if their face values lie between $u^c_{j+1/2}$ and $u^{up}_{j+1/2}$, and this is the case if ϕ is chosen so that $\phi(r) \in I(1,r)$. Observe that the UNO2 scheme corresponds to $\phi(r) = \min(1,r)$ and the Sonicbee, to $\phi(r) = \max(1,r)$.

The SONIC scheme corresponding to vanLeer's MUSCLE scheme can be obtained by simply defining $\phi(r) = (1/2)(1+r)$, or equivalently

$$u^{\phi}_{j+1/2} = \frac{1}{2}(u^c_{j+1/2} + u^{up}_{j+1/2}). \tag{2.26}$$

We name it the SONIC-A scheme ("A" for "average").

We conclude this section with the following remark. In defining $u^c_{j+1/2}$, the minmod function of eq.(2.17b) can be replaced by any TVD2 limiter function. One then comes up with a class of schemes which posesses all the properties of SONIC schemes and admits SONIC schemes as a subclass. We will report on this enlarged class elsewhere.

3. Conservation laws

Consider the following scalar conservation law

$$\frac{\partial u}{\partial t} + \frac{\partial f}{\partial x} = 0 \tag{3.1}$$

where f is a smooth convex function of u, that is, f lies above all its tangents. This implies that $a(u) = df/du$ is an increasing function of u. Let $\bar{u}$ be the unique sonic point of f, i.e., $a(\bar{u}) = 0$. Using the simple change of variables $v = u - \bar{u}$ and $g(v) = f(u) - f(\bar{u})$, one may assume without loss of generality that $\bar{u} = 0$ and $f(0) = 0$. The simplest conservation law with all the above properties is the inviscid Burgers' equation

$$\frac{\partial u}{\partial t} + \frac{1}{2}\frac{\partial u^2}{\partial x} = 0. \tag{3.2}$$

Equation (3.1) can be discretized in conservation form using the midpoint rule

$$u^{n+1}_j = u^n_j - \lambda(\tilde{f}_{j+1/2} - \tilde{f}_{j-1/2}) \tag{3.3}$$

where, again, $\lambda = \Delta t/\Delta x$ and $\tilde{f}_{j+1/2} = f(\tilde{u}_{j+1/2})$ and the tilde replaces the superscript $n+1/2$, e.g., $\tilde{u}_{j+1/2} = u^{n+1/2}_{j+1/2}$. For simplicity of the proofs, the CFL number μ is assumed to satisfy

$$\sup(\lambda|a(u)|) = \mu \leq 1/2$$

The main problem is to define the face value $\tilde{u}_{j+1/2}$. To avoid mixing up the numerics and the physics, we adopt the projection-evolution approach advocated by vanLeer [5].

The projection stage is purely numerics. First, assuming that the flow comes from the left, using the SONIC schemes of the previous section, one can define face value $u^L_{j+1/2}$. Then, on reversing the flow direction, a is now negative, one obtains $u^R_{j+1/2}$. This is the end of the projection stage.

In the evolution stage, physics enters. We have to decide the flow direction and define the face value $\tilde{u}_{j+1/2}$ properly. To do this, consider the following cases, (cf. section 6 of [2] and section 4 of [1])

1. $a^L_{j+1/2} > 0$ where $a^L_{j+1/2} = a(u^L_{j+1/2})$. This is equivalent to $u^L_{j+1/2} > 0$. We have two subcases:
   a. $a^R_{j+1/2} \geq 0$, then upwind direction corresponds to j;
   b. $a^R_{j+1/2} < 0$, we have a shock.
2. $a^L_{j+1/2} \leq 0$, equivalently $u^L_{j+1/2} \leq 0$. Again, we have two subcases:
   a. $a^R_{j+1/2} < 0$, then upwind direction corresponds to $j+1$;
   b. $a^R_{j+1/2} \geq 0$, we have a sonic expansion fan.

In order to prove the nonoscillatory property later, the definitions of $\tilde{u}_{j+1/2}$ below are somewhat different from those in the literature.

In case 1a above, assume that the approximations for u and a are linear in $[x_j, x_{j+1/2}]$. Then, using a characteristic argument,

$$\tilde{u}^L_{j+1/2} = u^L_{j+1/2} - \frac{a^L_{j+1/2}}{1 + \lambda(a^L_{j+1/2} - a_j)}\lambda(u^L_{j+1/2} - u_j). \tag{3.4}$$

The ratio in the above expression is a more accurate approximation to $\tilde{a}^L_{j+1/2}$. For Burgers' equation, $\tilde{u}^L_{j+1/2}$ is of the same sign as $u^L_{j+1/2}$. In general to assure that the sign has not been changed, with ϵ a small positive number (say, 10^{-9}), we define

$$\tilde{u}^L_{j+1/2} = \max(\epsilon, \tilde{u}^L_{j+1/2}) \tag{3.5}$$

$$\tilde{u}_{j+1/2} = \tilde{u}^L_{j+1/2} \tag{3.6}$$

Case 2a is similar to the above case with proper sign changes,

$$\tilde{u}^R_{j+1/2} = u^R_{j+1/2} + \frac{a^R_{j+1/2}}{1 + \lambda(-a^R_{j+1/2} + a_{j+1})}\lambda(u^R_{j+1/2} - u_{j+1}). \tag{3.7}$$

$$\tilde{u}^R_{j+1/2} = \min(-\epsilon, \tilde{u}^R_{j+1/2}) \tag{3.8}$$

$$\tilde{u}_{j+1/2} = \tilde{u}^R_{j+1/2} \tag{3.9}$$

In case 1b, we define $\tilde{u}^L_{j+1/2}$ and $\tilde{u}^R_{j+1/2}$ as in eqs. (3.4), (3.5) and (3.7), (3.8) respectively. The upwind direction depends on the sign of

$$A_{j+1/2} = (f(\tilde{u}^R_{j+1/2}) - f(\tilde{u}^L_{j+1/2}))/(\tilde{u}^R_{j+1/2} - \tilde{u}^L_{j+1/2}) \tag{3.10}$$

If $A_{j+1/2} \geq 0$, $\tilde{u}_{j+1/2}$ is obtained from eq. (3.6) and if $A_{j+1/2} < 0$, from eq. (3.9).

Case 2b for the sonic expansion fan is simple:

$$\tilde{u}_{j+1/2} = 0. \tag{3.11}$$

The above definitions of face values are consistent in the sense that if $\tilde{u}_{j+1/2} > 0$, then $u^L_{j+1/2} > 0$ and the flow comes from the left. Conversely, if $\tilde{u}_{j+1/2} < 0$, then $u^R_{j+1/2} < 0$ and the flow comes from the right. Finally, $\tilde{u}_{j+1/2} = 0$ corresponds to a sonic expansion fan where $u^L_{j+1/2} \leq 0$ and $u^R_{j+1/2} \geq 0$.

Next, we show that SONIC schemes defined as above are nonoscillatory. The case $\tilde{u}_{j+1/2} = \tilde{u}_{j-1/2}$ is trivial. Assuming that $\tilde{u}_{j+1/2} \neq \tilde{u}_{j-1/2}$, let

$$A_j = (f(\tilde{u}_{j+1/2}) - f(\tilde{u}_{j-1/2}))/(\tilde{u}_{j+1/2} - \tilde{u}_{j-1/2}), \tag{3.12}$$

then eq. (3.3) can be written in a form similar to (2.2)

$$u^{n+1}_j = u^n_j - A_j\lambda(\tilde{u}_{j+1/2} - \tilde{u}_{j-1/2}). \tag{3.13}$$

If $A_j = 0$ there is nothing to prove. Consider the case $A_j > 0$. Similar arguments hold for $A_j < 0$. To show that these schemes are nonoscillatory, it suffices to show that they have the quadratic upwind monotonic property (2.19) where upwind direction corresponds to index $j-1$ since $A_j > 0$. Indeed, with the CFL condition $\leq 1/2$, we only have to show

$$\tilde{u}_{j-1/2} \in I(u_{j-1}, u^c_{j-1/2}, u_j); \quad \tilde{u}_{j+1/2} \in I(u_j, u^{up}_{j+1/2}, u^{up2}_{j+1/2}). \tag{3.14a, b}$$

Notice that (3.14) is the same as (2.13) except that $u_{j-1/2}$ and $u_{j+1/2}$ are replaced by $\tilde{u}_{j-1/2}$ and $\tilde{u}_{j+1/2}$. We use the above restricted CFL condition here. In the nonlinear case, the solution is no longer given by the parabola P_j in the observation following (2.4) but by the straight line $\tilde{U}_{j-1/2}\tilde{U}_{j+1/2}$. Condition (3.14a) follows from the definition of face values. As for condition (3.14b), if $\tilde{u}_{j+1/2} > 0$, then the consistency arguments after eq. (3.11) assert that at face $x_{j+1/2}$, the flow comes from the left, thus the above claim. Before considering the case $\tilde{u}_{j+1/2} \leq 0$, we make an essential observation. Condition (3.14b) can be replaced by the following condition and (2.19) still holds:

$$\tilde{u}_{j+1/2} \in I(\tilde{u}_{j-1/2}, \tilde{u}^L_{j+1/2}). \tag{3.15}$$

See Fig. 6(A). Next, if $\tilde{u}_{j+1/2} = 0$, then from the consistency arguments, $\tilde{u}^L_{j+1/2} \leq 0$. In order that $A_j > 0$, $\tilde{u}_{j-1/2} > 0$ (Fig. 6(B)). Since $\tilde{u}_{j+1/2} = 0$, it lies between $\tilde{u}_{j-1/2}$ and $\tilde{u}^L_{j+1/2}$ which is (3.15). Finally, we consider the case $\tilde{u}_{j+1/2} < 0$, i.e., in the control interval $[x_{j-1/2}, x_{j+1/2}]$ there is a

shock since $\tilde{u}_{j-1/2} > 0$ (Fig. 6(C)). The difficulty here is that $\tilde{u}_{j+1/2} = \tilde{u}^R_{j+1/2}$ and yet we must show that (3.15) holds true. We need another definition.

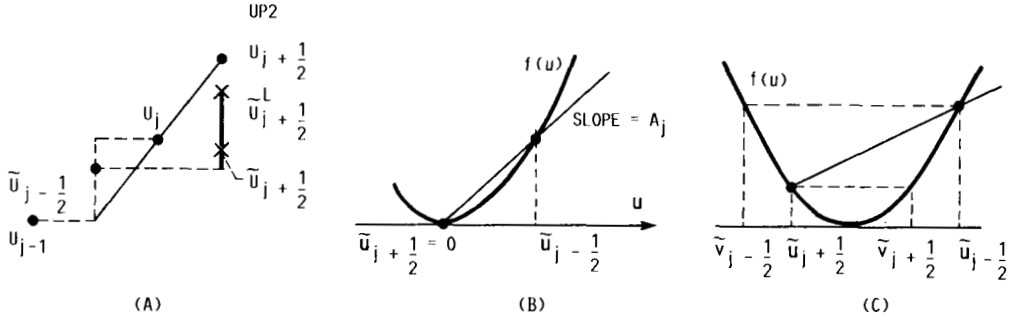

FIGURE 6.

For each u, let v be of opposite sign such that $f(v) = f(u)$. In the case of Burgers' equation, $v = -u$. Because of the assumption that $A_j > 0$,

$$\tilde{v}_{j-1/2} < \tilde{u}_{j+1/2} < 0 < \tilde{v}_{j+1/2} < \tilde{u}_{j-1/2}. \tag{3.16}$$

Rewrite (3.12) and (3.13) with $\tilde{u}_{j+1/2}$ replaced by $\tilde{v}_{j+1/2}$:

$$\tilde{A}_j = (f(\tilde{v}_{j+1/2}) - f(\tilde{u}_{j-1/2}))/(\tilde{v}_{j+1/2} - \tilde{u}_{j-1/2}), \tag{3.17}$$

$$u_j^{n+1} = u_j^n - \tilde{A}_j \lambda (\tilde{v}_{j+1/2} - \tilde{u}_{j-1/2}). \tag{3.18}$$

Observe that $\tilde{A}_j \lambda$ is within the above CFL bound since $0 \le \tilde{A}_j \le a_{j-1/2}$. Thus instead of (3.15) it suffices to show that

$$\tilde{v}_{j+1/2} \in I(\tilde{u}_{j-1/2}, \tilde{u}^L_{j+1/2}). \tag{3.19}$$

If $\tilde{u}^L_{j+1/2} \le 0$, (3.19) follows from (3.16). If $\tilde{u}^L_{j+1/2} > 0$, we have a shock at face $x_{j+1/2}$ and since the flow comes from the right,

$$\tilde{u}_{j+1/2} = \tilde{u}^R_{j+1/2} < 0 < \tilde{u}^L_{j+1/2} < \tilde{v}_{j+1/2}.$$

The last inequality above and the last one in (3.16) implies (3.19). This completes the proof.

4. Computational results

In the first set of problems, we present computational results for advection with constant speed. The initial profiles consist of a $\sin^2$ wave, a square wave, a triangular wave and a semi-ellipse wave. Each wave contains 20 grid points on a uniform grid of 200 points. Using periodic boundary conditions, the profile is advected one period with CFL number 0.5. The results after 400 time steps are shown in Figs. 7 (A) for Minmod, (B) for UNO2, (C) for MUSCLE, (D) for SONIC-A, (E) for

Superbee, and (F) for Sonicbee schemes. The figures on the left correspond to TVD schemes, and those on the right, to SONIC schemes. One can observe that the SONIC schemes are more accurate than their TVD counterparts. The Minmod scheme, and to a lesser degree, the UNO2 scheme are somewhat diffusive. The Sonicbee scheme can resolve the square wave and the triangular wave very accurately, however, it shares the compressive character of the Superbee scheme in the semi-ellipse wave and it has an overshoot in the $\sin^2$ wave. The SONIC-A scheme appears to be the best of the schemes tested. Although it does not resolve the square wave as sharply as the Superbee and the Sonicbee schemes, it gives accurate solutions to the other three waves.

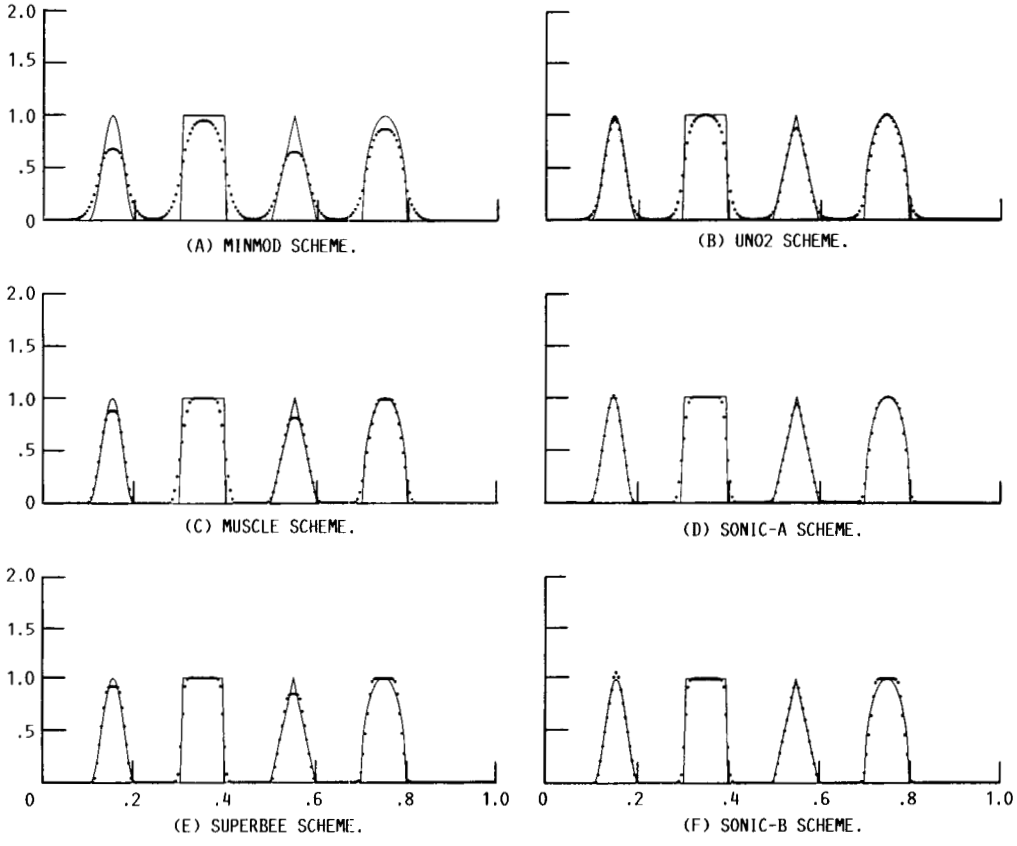

FIGURE 7. - COMPARISON OF TVD (LEFT) AND SONIC (RIGHT) SCHEMES.

In the second set of problems, results for Burgers' equation are presented. The initial condition is a sine wave of 20 grid points in the interval $[-1, 1]$. The dots represent the numerical solutions and the curves, the exact solutions. With CFL number 0.5 and periodic boundary conditions, highly accurate results at time $t = 0.4$ are obtained in Figs. 8 (A) for UNO2, (B) for SONIC-A, and (C) for Sonicbee schemes. Observe that a shock has formed at $x = \pm 1$ and the solutions have no oscillations. The SONIC-A scheme is slightly more accurate than the UNO2 and the

Sonicbee schemes in this case.

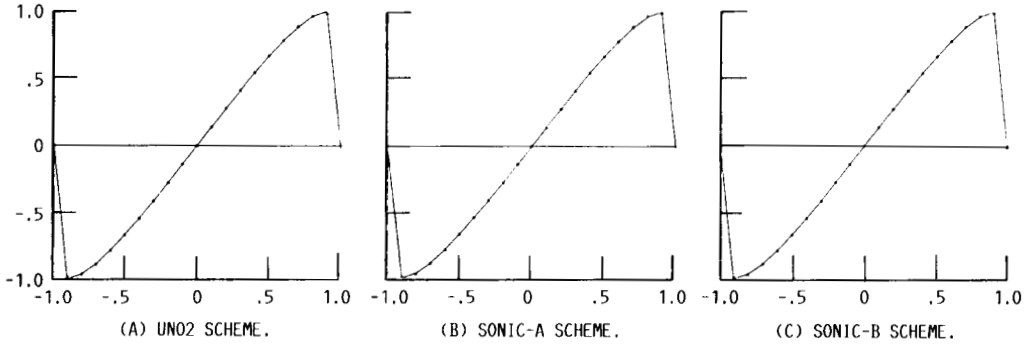

(A) UNO2 SCHEME. (B) SONIC-A SCHEME. (C) SONIC-B SCHEME.

FIGURE 8. - NUMERICAL SOLUTIONS FOR BURGERS' EQUATION, t = 0.4.

5. Conclusion

We have introduced the concept of upwind monotonicity which was used to show that the new class of schemes, named SONIC, is nonoscillatory and second-order accurate.

Acknowledgments

The author wishes to thank Drs. S. C. Chang, J. E. Lavery and M. S. Liou for their helpful suggestions in preparing this paper.

References

1. A. Harten, B. Engquist, S. Osher & S. R. Chakravarty, "Uniformly high-order accurate nonoscillatory schemes. III," *J. Comp. Phys.* **71**(1987), 231-303.
2. A. Harten & S. Osher, "Uniformly high-order accurate nonoscillatory schemes. I," *SIAM J. Numer. Anal.* **24**(1987), 279-309.
3. R. Sanders, "A third-order accurate variation nonexpansive difference scheme for single nonlinear conservation laws," *Math. Comp.* **51**(1988), 535-558
4. P. K. Sweby, "High resolution schemes using flux limiters for hyperbolic consevation laws," *SIAM J. Numer. Anal.* **21**(1984), 995-1011.
5. B. vanLeer, "Towards the ultimate conservative difference scheme. IV. A new approach to numerical convection," *J. Comp. Phys.* **23**(1977), 276-298.
6. B. vanLeer, "Towards the ultimate conservative difference scheme. V. A second-order Sequel to Godunov's method," *J. Comp. Phys.* **32**(1979), 101-136.

NASA
National Aeronautics and Space Administration

Report Documentation Page

1. Report No.	2. Government Accession No.	3. Recipient's Catalog No.
NASA TM-102010		

4. Title and Subtitle	5. Report Date
Second-Order Accurate Nonoscillatory Schemes for Scalar Conservation Laws	6. Performing Organization Code

7. Author(s)	8. Performing Organization Report No.
Hung T. Huynh	E-4721
	10. Work Unit No. 505-62-21

9. Performing Organization Name and Address	11. Contract or Grant No.
National Aeronautics and Space Administration Lewis Research Center Cleveland, Ohio 44135-3191	13. Type of Report and Period Covered Technical Memorandum

12. Sponsoring Agency Name and Address	14. Sponsoring Agency Code
National Aeronautics and Space Administration Washington, D.C. 20546-0001	

15. Supplementary Notes

Prepared for the 6th International Conference on Numerical Methods in Laminar and Turbulent Flow cosponsored by the University College of Swansea, UK, Office of Naval Research Branch Office London, Journal for Numerical Methods in Fluids, International Journal for Engineering Computations, and International Journal for Artificial Intelligence Swansea, United Kingdom, July 11-15, 1989.

16. Abstract

A new class of explicit finite-difference schemes for the computation of weak solutions of nonlinear scalar conservation laws is presented and analyzed. These schemes are uniformly second-order accurate and nonoscillatory in the sense that the number of extrema of the discrete solution is not increasing in time.

17. Key Words (Suggested by Author(s))	18. Distribution Statement
Second-order accurate Nonoscillatory schemes Scalar conservation laws	Unclassified - Unlimited Subject Category 02

19. Security Classif. (of this report)	20. Security Classif. (of this page)	21. No of pages	22. Price*
Unclassified	Unclassified	16	A03

NASA FORM 1626 OCT 86

*For sale by the National Technical Information Service, Springfield, Virginia 22161